Research Square

Preprints are preliminary reports that have not undergone peer review.
They should not be considered conclusive, used to inform clinical practice,
or referenced by the media as validated information.

Proteome analysis of the Gram-positive fish pathogen Renibacterium salmoninarum reveals putative role of membrane vesicles in virulence

Tobias Kroniger
Institute of Microbiology, Department of Microbial Proteomics, Center for Functional Genomics of Microbes, University of Greifswald, 17489 Greifswald

Daniel Flender
Institute of Microbiology, Department of Microbial Proteomics, Center for Functional Genomics of Microbes, University of Greifswald, 17489 Greifswald

Rabea Schlüter
Imaging Center of the Department of Biology, University of Greifswald, 17489 Greifswald

Bernd Köllner
Institute of Immunology, Friedrich-Loeffler-Institute, Federal Research Institute for Animal Health, 17493 Greifswald - Isle of Riems

Anke Trautwein-Schult
Institute of Microbiology, Department of Microbial Proteomics, Center for Functional Genomics of Microbes, University of Greifswald, 17489 Greifswald

Dörte Becher (dbecher@uni-greifswald.de)
Institute of Microbiology, Department of Microbial Proteomics, Center for Functional Genomics of Microbes, University of Greifswald, 17489 Greifswald

Research Article

Keywords: bacterial kidney disease (BKD), MV fraction, lipoproteins, membrane vesicles (MVs), nucleic acids, peptidoglycan

Posted Date: July 26th, 2021

DOI: https://doi.org/10.21203/rs.3.rs-744942/v1

License: This work is licensed under a Creative Commons Attribution 4.0 International License.
Read Full License

Proteome analysis of the Gram-positive fish pathogen *Renibacterium salmoninarum* reveals putative role of membrane vesicles in virulence

Tobias Kroniger[1], Daniel Flender[1], Rabea Schlüter[2], Bernd Köllner[3], Anke Trautwein-Schult[1] and Dörte Becher[1,*]

[1]Institute of Microbiology, Department of Microbial Proteomics, Center for Functional Genomics of Microbes, University of Greifswald, 17489 Greifswald, Germany

[2]Imaging Center of the Department of Biology, University of Greifswald, 17489 Greifswald, Germany

[3]Institute of Immunology, Friedrich-Loeffler-Institute, Federal Research Institute for Animal Health, 17493 Greifswald - Isle of Riems, Germany

[*]dbecher@uni-greifswald.de

Abstract

The bacterial kidney disease (BKD) is a chronic bacterial disease affecting both wild and farmed salmonids. The causative agent for BKD is the Gram-positive fish pathogen *Renibacterium salmoninarum*. As treatment and prevention of BKD has proven to be difficult, it is important to know and identify the key bacterial proteins that interact with the host. We used subcellular fractionation to report semi-quantitative data for the cytosolic, membrane, extracellular and membrane vesicle (MV) proteome of *R. salmoninarum*. These data can aid as a backbone for more targeted experiments regarding the development of new drugs for the treatment of BKD. Further analysis was focused on the MV proteome, where both major immunosuppressive proteins P57/Msa and P22 and proteins involved in bacterial adhesion were found in high abundance. Interestingly, the P22 protein was enriched only in the extracellular and MV fraction, implicating that MVs may play a role in host-pathogen interaction. Compared to the other subcellular fractions, the MVs were also enriched in lipoproteins and all four cell wall hydrolases belonging to the New Lipoprotein C/Protein of 60 kDa (NlpC/P60) family were detected, suggesting an involvement in the formation of the MVs.

Introduction

Renibacterium salmoninarum is a 0.8-2 µm long, encapsulated, rod shaped, non-motile Gram-positive fish pathogen that is the causative agent of the bacterial kidney disease (BKD) in salmonids. Treatments for BKD have proven to be difficult as the pathogen is able to invade the hosts macrophages and survive and replicate intracellularly[1,2]. Further, the transmission of *R. salmoninarum* can occur vertically from parent to progeny via the egg[3] and horizontally from fish to fish, e.g. via the fecal-oral route[4]. BKD has an impact on the sustainable production of salmonids for consumption[5] where economic losses with up to 80% of *Oncorhyncus spp.* and 40% of *Salmo salar* stocks have been described[6]. While the processes during the pathogenicity of *R. salmoninarum* are not fully understood, several proteins are reported to be involved in the virulence of the bacterium. The immunogenic extracellular major soluble antigen of 57 kDa P57/Msa is widely considered as the dominant virulence factor of *R. salmoninarum* as the virulence of the bacterium correlates with the amount of the P57/Msa protein associated with the bacterial cell surface[7] and also with the number of encoded gene copies of *msa*[8]. A second major virulence protein that is reported to be involved in immunosuppression of the host is a surface protein of 22 kDa named P22[9,10]. Both, P57/Msa and P22 are implicated in the suppression of the host antibody production and agglutination of leucocytes[9,11]. Other proteins that are involved in the virulence of *R. salmoninarum* include iron acquisition proteins[12], hemolysins[13,14], metalloproteases[14], sortase and adhesion proteins[15], capsular synthesis proteins[14], catalase[2,14], superoxide dismutase[14] and thioredoxin peroxidases[14].

For rational vaccine designs it is crucial to identify the proteins that might be involved in host-pathogen interaction and to know their subcellular localization. For example, proteins located in the bacterial membrane (e.g. lipoproteins) or secretory proteins which directly interact with host cells are good targets for the development of vaccines[16,17]. While the translocation of bacterial proteins is typically mediated by the Sec or Tat secretion pathway or the more dedicated type I-V protein secretion systems[18], proteins can also be secreted via bacterial membrane vesicles (MVs). Bacterial MVs are spherical extracellular bubbles known to be shed from Gram-negative and Gram-positive bacterial cell membranes and range in size between 20 and 400 nm[19]. While the mechanism behind the formation of MVs in Gram-positive bacteria is not fully understood, proteins involved in cell wall modification, like transpeptidases and autolysins are hypothesized to play an important role in the formation process, as these proteins have been detected in MVs released from Gram-positive bacteria[20–22]. Other contents of MVs include lipopolysaccharides[23], peptidoglycan[24], nucleic acids[24], toxins[25] and proteins[26,27]. Some of the proteins identified in MVs were shown to be relatively enriched within the MVs when compared to their parent bacterium, suggesting a selective packing of proteins into the MVs[26,27]. Similar to MVs of Gram-negative bacteria, MVs of Gram-positive bacteria and their cargo are reported to be involved in numerous processes[28] including virulence[29]. The various contents of MVs and the presentation of

putative immunogenic membrane proteins in a lipid environment[30] make MVs a promising platform for vaccine development[21].

Here, the first comprehensive proteomic study of *R. salmoninarum* and their MVs was performed. By using subcellular fractionation, semi-quantitative proteome data with an in-depth view on proteins involved in virulence is reported. The global investigation of the most abundant proteins in different subcellular localizations may provide an insight for vaccine or drug development research and give hints regarding the biogenesis of MVs in *R. salmoninarum* or in Gram-positive bacteria.

Results

Overall identifications and overlap between subcellular fractions

This study is the first comprehensive proteome analysis of the *R. salmoninarum* strain ATCC 33209. By using subcellular fractionation, 1,781 of the 3,421 annotated proteins of *R. salmoninarum* were identified. Of these 1,781 identified proteins, 1,674 proteins were label-free quantified in at least 3 out of the 4 biological replicates, resulting in a quantification efficiency of 93.9%. A principal component analysis (PCA) of the label-free quantification (LFQ) intensities revealed a distinct differentiation between the four enriched subcellular fractions and a high reproducibility between the replicates within the respective fractions (Fig. 1a). Most proteins were quantified in the membrane fraction (1,540 proteins) followed by the cytosol (1,243), extracellular (818) and the MV fraction (146) (Fig. 1b). Several proteins were exclusively detected in one of the subcellular fractions. The highest number of exclusively quantified proteins were observed in the membrane fraction (321), followed by the cytosol (61), extracellular (48) and the MV fraction (1). To investigate an experimental enrichment of proteins and also to validate the success of the subcellular fractionation, the theoretical protein localizations were predicted *in silico* by using the tool PSORTb (version v3.0.2)[31]. For the annotated proteome of *R. salmoninarum*, the theoretical protein localizations were discriminated between "unknown" (781 total proteins), "cytoplasmic" (1,527), "cytoplasmic membrane" (1,035), "cell wall" (15) and "extracellular" (63) (Supplementary Table). A comparison between these theoretical protein localizations and the observed experimental protein localization in the enriched subcellular fraction demonstrated that proteins predicted to be cytosolic were enriched in quality and quantity in the cytosol and membrane fraction, but only some of these proteins were identified in a relative low abundance within the extracellular and MV fraction (Fig. 1c). Further, in comparison to the cytosol fraction, a successful enrichment of membrane proteins was detected in the membrane fraction, as more membrane proteins were identified and these were relatively more abundant. The most abundant proteins in the extracellular and MV fraction were primarily predicted to be of unknown, membrane or extracellular localization. Additionally, the presence of different secretion signal peptides was predicted by using the tool SignalP (version 5.0)[32]. According to the results of SignalP, 3,187 proteins in the proteome of *R. salmoninarum* are predicted to have no signal peptide ("Other"), 136 proteins are predicted to be Sec substrates cleaved by SPase I ("Sec/SPI"), 78 lipoproteins are Sec substrates cleaved by SPase II ("Lipo/SPII") and 20 proteins are predicted to be Tat substrates cleaved by SPase I ("Tat/SPI"). These predictions were again matched with the findings of the mass spectrometry results. While the most abundant proteins in the cytosol and membrane fraction were without any signal peptide, proteins with a Sec/SPI and Lipo/SPII secretion signal were slightly enriched in quality and quantity in the membrane fraction compared to the cytosol fraction (Fig. 1d).

In the extracellular fraction a clear enrichment of proteins with a Sec/SPI secretion signal was observed. Whereas only 6.1% (50/818) of the detected proteins were predicted to have this secretion signal, these proteins accounted for roughly 2/3 of the protein amount in this fraction. Proteins with a Sec/SPI secretion signal were also high abundant in the MV fraction. Further, compared to the other subcellular fractions, similar amounts of proteins with Lipo/SPII secretion signal were identified in the MV fraction, but quantitatively a relative enrichment of these proteins was observed. Tables of the total identified proteins, the identifications in each of the subcellular fractions, the exclusive protein identifications in each of the subcellular fractions as well as the used PSORTb and SignalP predictions for the *R. salmoninarum* proteome can be found in Supplementary Table.

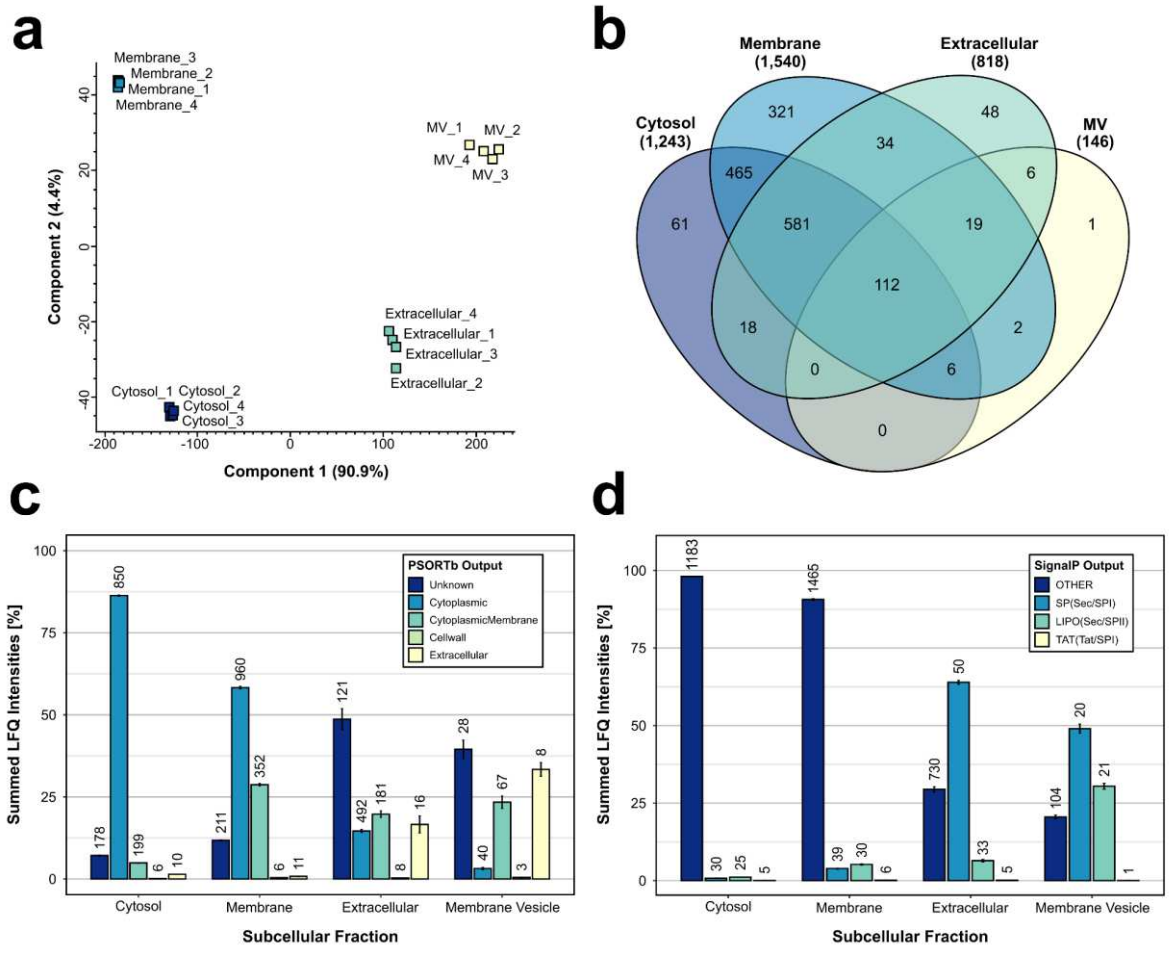

Figure 1: Overview of the protein identifications, predicted protein localizations and predicted signal peptides for all enriched subcellular fractions: **(A)** Principal component analysis of the enriched subcellular fractions. Missing values were imputed from normal distribution of each replicate (MV = membrane vesicle); **(B)** Overview of the overlap and the exclusively quantified proteins between the four enriched subcellular fractions (MV = membrane vesicle); **(C)** Illustration of the summed LFQ intensities of quantified proteins in the four subcellular fractions assigned to the respective predicted PSORTb localizations. The number of quantified proteins with the respective PSORTb prediction in each of the subcellular fractions is indicated above the bars; **(D)** Illustration of the summed LFQ intensities of quantified proteins in the four subcellular fractions assigned to the predicted SignalP protein signal peptides. The number of quantified proteins with the respective SignalP signal peptide prediction within the subcellular fractions is indicated above the bars.

Subcellular enrichments of proteins involved in host-pathogen interaction

For the understanding of the host-pathogen interaction, the analysis of secreted proteins and proteins associated with the surface of the bacterium are crucial. This analysis may further be important for new targeted approaches in drug development as inhibition of important proteins involved in host-pathogen interaction may lead to new treatment methods for BKD. The applied method of the subcellular fractionation provides information on the localization of proteins potentially involved in virulence and their relative abundance within the respective subcellular fraction. For a relative comparison of the protein amounts within the respective fractions, the LFQ intensities were median normalized within each of the subcellular fractions to take the enrichment effects during the sample preparation into account (Supplementary Table). The median normalization allows relative comparison between the subcellular fractions and can demonstrate enrichment effects of proteins in the fractions. Overall, 25 proteins that are associated with virulence processes were grouped and analyzed according to their high abundant occurrence in all, three, two or only one of the enriched subcellular fractions (Fig. 2, Table 1).

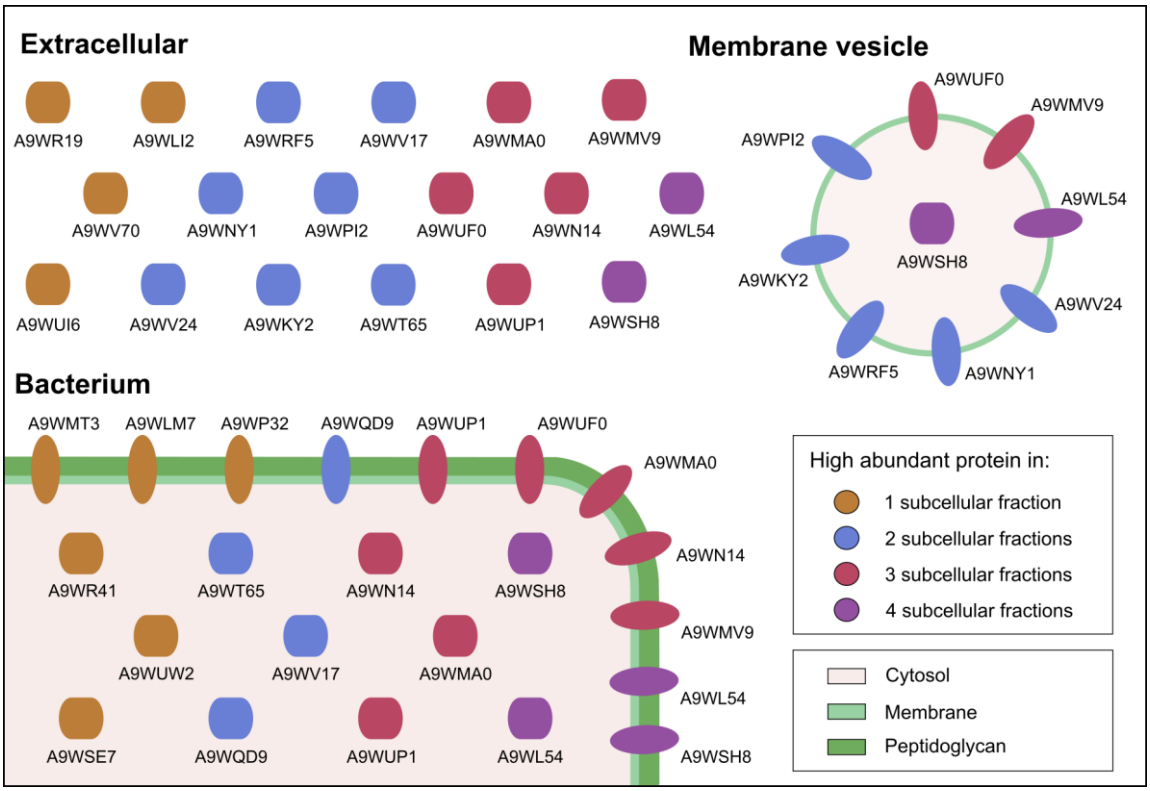

Figure 2: Schematic visualization of 25 high abundant proteins that are involved in virulence processes of *R. salmoninarum* and their experimental subcellular localization. Proteins are colored depending on their high abundance (higher than a log2 transformed median normalized LFQ intensity of 2) in one or more of the enriched subcellular fractions. Proteins are marked with their UniProt identifier.

147 The quantitative analysis of these 25 proteins within the subcellular fractions revealed that some
148 proteins were only high abundant in the cytosolic (UniProt ID A9WUW2; A9WR41; A9WSE7),
149 membrane (A9WMT3; A9WLM7; A9WP32) or extracellular fraction (A9WV70; A9WR19; A9WLI2;
150 A9WUI6). Other proteins were found in high abundance in both the cytosolic and membrane
151 (A9WQD9), cytosolic and extracellular (A9WV17; A9WT65) or the extracellular and MV fraction
152 (A9WKY2; A9WPI2; A9WRF5; A9WV24; A9WNY1). In addition, some proteins were detected in
153 three of the subcellular fractions. The chaperonins 1 and 2 (A9WMA0; A9WN14) and a negative
154 regulator of genetic competence (A9WUP1) were found in high abundance in the cytosolic, membrane
155 and extracellular fraction but not in the MVs. Additionally, a ferric enterobactin transport system
156 (A9WMV9) and a cell wall endopeptidase (A9WUF0) were enriched in the membrane, extracellular
157 and MV fraction, but not in the cytosol. Two of the 25 proteins have also been identified with high
158 abundance in all four subcellular fractions. The most abundant protein of these two proteins is the cell
159 surface protein P57/Msa (A9WL54), which is reported to be the major virulence factor of
160 *R. salmoninarum*[7,11,33]. The other protein is a FK506 binding protein (FKBP) type peptidylprolyl
161 isomerase (PPIase) (A9WSH8).

162

Table 1: 25 high abundant proteins that are involved in virulence of *R. salmoninarum* and their subcellular localization. Proteins are listed in the table below with their predicted PSORTb localizations (U = unknown; C = cytoplasmic; CM = cytoplasmic membrane; E = extracellular), their predicted SignalP signal peptides (SP = secretory signal peptides transported by the Sec translocon and cleaved by Signal Peptidase I; Lipo = lipoprotein signal peptides transported by the Sec translocon and cleaved by Signal Peptidase II; OTHER = no detectable signal peptide) and the mean log2 transformed median normalized LFQ intensities in the four enriched subcellular fractions with their standard deviation in between replicates (n = 4; Cyt = cytosol, Mem = membrane, Extra = extracellular, MV = membrane vesicles). Proteins are grouped and colored depending on their high abundance (higher than a log2 transformed median normalized LFQ intensity of 2) in one or more of the enriched subcellular fractions. Within the groups, the listed proteins are sorted according to their theoretical subcellular localization.

	UniProt ID	Gene	Protein name	PSORTb	SignalP	Median normalized log_2 LFQ intensities			
						Cytosol	Membrane	Extra	MV
	A9WSH8	RSal33209_2033	Peptidylprolyl isomerase	C	Lipo	**3.66 ± 0.03**	**4.97 ± 0.27**	**4.54 ± 0.48**	**4.19 ± 0.53**
	A9WL54	msa1	Cell surface protein	U	SP	**3.64 ± 0.10**	**5.00 ± 0.25**	**10.85 ± 0.21**	**7.08 ± 0.43**
	A9WMA0	groL1	60 kDa chaperonin 1 (GroEL protein 1)	C	Other	**7.47 ± 0.07**	**6.66 ± 0.10**	**5.16 ± 0.18**	-1.20 ± 0.54
	A9WN14	groL2	60 kDa chaperonin 2 (GroEL protein 2)	C	Other	**6.70 ± 0.09**	**4.86 ± 0.08**	**4.34 ± 0.12**	
	A9WUP1	RSal33209_3195	Negative regulator of genetic competence	C	Other	**2.12 ± 0.09**	**3.61 ± 0.08**	**2.89 ± 0.09**	-0.63 ± 0.35
	A9WMV9	RSal33209_1684	Ferric enterobactin transport system	CM	Lipo	0.62 ± 0.09	**2.85 ± 0.26**	**5.80 ± 0.09**	**4.89 ± 0.44**
	A9WUF0	RSal33209_3103	Cell wall endopeptidase	E	SP	-0.07 ± 0.09	**3.51 ± 0.34**	**10.15 ± 0.58**	**8.01 ± 0.52**
	A9WQD9	RSal33209_0845	Catalase	C	Other	**5.93 ± 0.05**	**2.39 ± 0.13**	1.93 ± 0.20	
	A9WV17	RSal33209_3326	6-phosphogluconate dehydrogenase	C	Other	**3.39 ± 0.09**	0.88 ± 0.07	**4.52 ± 0.20**	
	A9WKY2	RSal33209_0501	NLPC_P60 domain containing protein	CM	SP	-4.73 ± 0.10	-0.12 ± 0.60	**7.31 ± 0.72**	**4.44 ± 0.50**
	A9WPI2	RSal33209_1229	Lipoprotein	CM	Lipo	-0.51 ± 0.13	1.79 ± 0.17	**3.64 ± 0.14**	**4.97 ± 0.36**
	A9WRF5	RSal33209_2511	Putative endopeptidase lytE	E	SP	-2.80 ± 0.17	1.41 ± 0.43	**8.64 ± 0.35**	**6.74 ± 0.15**
	A9WT65	RSal33209_2272	Superoxide dismutase	E	Other	**4.86 ± 0.05**	-0.17 ± 0.11	**2.64 ± 0.42**	
	A9WV24	RSal33209_3334	Uncharacterized protein	U	SP		-0.45 ± 0.47	**9.51 ± 0.15**	**7.70 ± 0.66**
	A9WNY1	RSal33209_1037	Trypsin-like serine protease	U	SP	-3.28 ± 0.31	-2.26 ± 0.68	**11.02 ± 0.54**	**5.39 ± 0.38**
	A9WMT3	RSal33209_1692	Siderophore biosynthesis protein	C	Other	-0.42 ± 0.03	**4.13 ± 0.07**	-0.19 ± 0.39	
	A9WV70	RSal33209_3381	Chitooligosaccharide deacetylase	C	SP	-3.84 ± 0.21	1.04 ± 0.13	**3.95 ± 0.54**	
	A9WUW2	clpP.3	ATP-dependent Clp protease	C	Other	**3.80 ± 0.18**	0.34 ± 0.12	1.33 ± 0.30	
	A9WR41	RSal33209_0015	Peptidyl-prolyl cis-trans isomerase	C	Other	**3.15 ± 0.27**	0.31 ± 0.25	1.29 ± 0.44	
	A9WSE7	RSal33209_2002	Probable transcriptional regulatory protein	C	Other	**3.00 ± 0.15**	0.96 ± 0.31	1.62 ± 0.23	
	A9WLM7	RSal33209_0050	Two-component response regulator	C	Other	1.94 ± 0.12	**2.99 ± 0.09**	1.43 ± 0.15	
	A9WR19	RSal33209_0646	Putative transcriptional regulator	CM	Other	-1.97 ± 0.17	0.31 ± 0.15	**6.91 ± 0.24**	
	A9WP32	ftsY	Signal recognition particle receptor FtsY	CM	Other	0.48 ± 0.08	**4.10 ± 0.13**	0.41 ± 0.21	
	A9WLI2	RSal33209_0186	Serpin (Serine proteinase inhibitor)	CM	Lipo			**2.13 ± 0.55**	
	A9WUI6	RSal33209_3139	Chitosanase	E	SP			**6.33 ± 0.82**	

The mentioned results illustrate major differences in protein abundancies between the enriched subcellular fractions. The major differences in between the fractions emphasize the importance of proteins such as P57/Msa (A9WL54) for the bacterium that are identified throughout all subcellular fractions in high abundance. Further, some proteins were enriched in similar subcellular fractions. For example, while the chaperonin 2 (A9WN14) was abundant in the cytosol, membrane and extracellular fraction, it was not detected in the MVs, indicating that this protein was neither actively sorted into the

MVs nor it was present at the MV formation site. Further, correlations in protein enrichments between the extracellular and MV fractions can be observed, as many proteins like the immunosuppressive P22 protein were enriched in the MVs and in the extracellular fraction (Table 1). Nevertheless, other proteins like the chitin degrading proteins A9WV70 and A9WUI6 or a serpin (A9WLI2) were detected in high quantity in the extracellular fraction and were not detected in the MVs, demonstrating that the correlations of the MV proteome with the secretome are not an effect of the subcellular fractionation.

Membrane vesicle proteome

The enriched and purified MVs of *R. salmoninarum* that were used for the MV proteome analysis ranged roughly in size between 20 and 100 nm (Fig. 3). In total, by using the above described method to get distinct subcellular protein fractions, 146 proteins were found to be associated with the MVs. Remarkably, only 40 of these proteins were predicted to be cytosolic. The other proteins were mainly predicted to be membrane proteins (67 proteins) or of unknown localization (28) (Fig. 1c). Furthermore, the MVs were quantitatively enriched in lipoproteins compared to the other subcellular fractions (Fig. 1d) and 11 of the 30 most abundant proteins in the MVs were lipoproteins (Table 2).

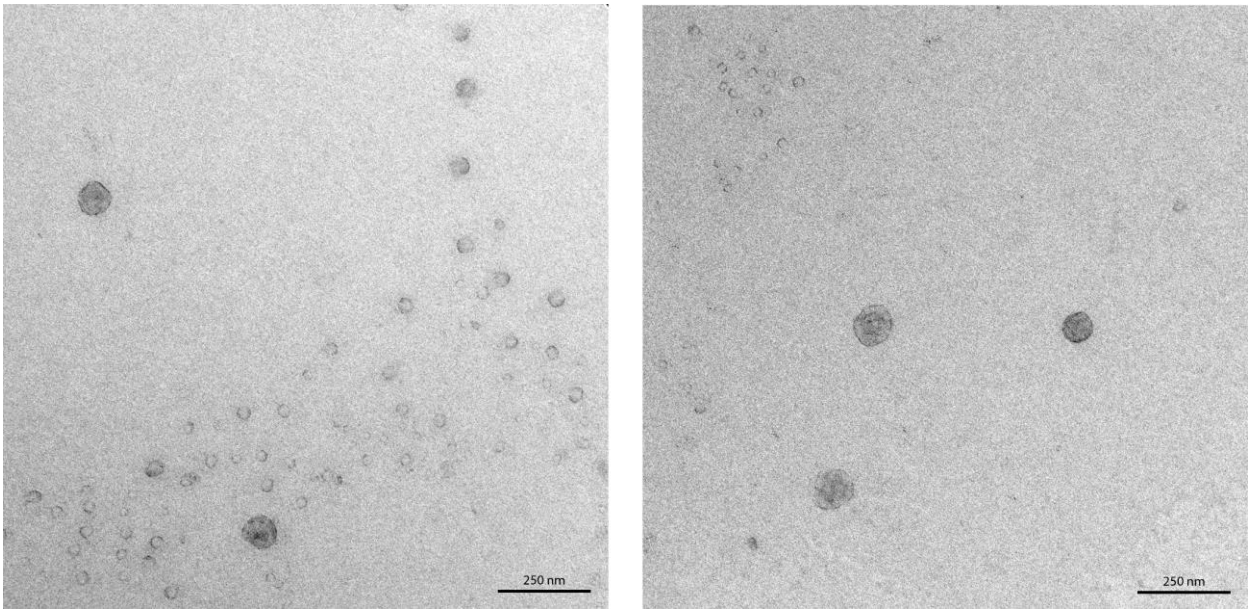

Figure 3: Transmission electron micrographs of isolated and purified membrane vesicles of *R. salmoninarum*.

The most abundant protein found in the vesicles was the cell wall endopeptidase (A9WUF0), which belongs to the cell wall hydrolyzing New Lipoprotein C/Protein of 60 kDa (NlpC/P60) protein family (Table 2). Interestingly, the MV fraction was the only subcellular fraction in which all four NlpC/P60 proteins of *R. salmoninarum* (A9WUF0; A9WKY1; A9WKY2; A9WVI9) were identified. The second

most abundant protein in the vesicles was the immunosuppressive P22 protein (A9WV24). The major virulence protein P57/Msa (A9WL54) was also in the top 5 most abundant proteins detected in the MVs. In addition, several transporters, proteases and two proteins belonging to the LytR protein family were found high abundant within the MVs.

Table 2: The 30 most abundant proteins quantified in the membrane vesicle (MV) fraction of *R. salmoninarum*. Proteins are listed according to their UniProt-ID and annotated protein name, their predicted PSORTb localizations (U = unknown; C = cytoplasmic; CM = cytoplasmic membrane; CW = cell wall; E = extracellular), their signal peptides predicted by SignalP (SP = secretory signal peptides transported by the Sec translocon and cleaved by Signal Peptidase I; LIPO = lipoprotein signal peptides transported by the Sec translocon and cleaved by Signal Peptidase II; OTHER = no detectable signal peptide) and sorted by their mean log2 transformed LFQ intensities in the MV fractions (n=4).

Protein ID	Protein Name	PSORTb	SignalP	LFQ MEAN
A9WUF0	Cell wall endopeptidase	E	SP	26.85 ± 0.26
A9WV24	Uncharacterized protein	U	SP	26.54 ± 0.52
A9WUM2	Phosphate-binding protein PstS	E	LIPO	26.12 ± 0.26
A9WPE4	Oligopeptide-binding protein	U	OTHER	26.07 ± 0.28
A9WL54	Cell surface protein	U	SP	25.92 ± 0.16
A9WRF5	Putative endopeptidase lytE	E	SP	25.58 ± 0.23
A9WPC8	Glycine betaine-binding protein	U	LIPO	25.32 ± 0.56
A9WRF2	Uncharacterized protein	CM	LIPO	25.2 ± 0.38
A9WSK5	Putative Iron(III) dicitrate-binding protein	CM	LIPO	25.01 ± 0.12
A9WLX2	Serine protease C	E	SP	24.4 ± 0.6
A9WNY1	Trypsin-like serine protease	U	SP	24.23 ± 0.2
A9WPI2	Lipoprotein	CM	LIPO	23.8 ± 0.14
A9WMV9	Ferric enterobactin transport system	CM	LIPO	23.72 ± 0.27
A9WM96	LytR_C domain-containing protein	CM	OTHER	23.42 ± 0.21
A9WKY2	NLPC_P60 domain-containing protein	CM	SP	23.27 ± 0.38
A9WSH8	Peptidylprolyl isomerase	C	LIPO	23.03 ± 0.25
A9WNV6	ABC transporter, permease protein	CM	OTHER	22.96 ± 0.32
A9WRT3	ABC transporter amino acid-binding protein	U	LIPO	22.7 ± 0.3
A9WP50	Signal peptidase I	CM	OTHER	22.44 ± 0.14
A9WR36	Hypothetical membrane protein	CM	OTHER	22.4 ± 0.52
A9WTJ9	Penicillin-insensitive transglycosylase	CM	OTHER	22.15 ± 0.42
A9WKU3	DsbA oxidoreductase	CW	LIPO	21.74 ± 0.56
A9WSE1	Protein-export membrane protein SecF	CM	OTHER	21.66 ± 0.42
A9WMK9	Cytochrome aa3 subunit 2	CM	LIPO	21.66 ± 0.48
A9WU60	Hypothetical exported protein	U	OTHER	21.65 ± 0.47
A9WLW9	Secretory peptidase	U	LIPO	21.56 ± 0.32
A9WSX9	DNA-directed RNA polymerase subunit beta'	C	OTHER	21.32 ± 0.28
A9WU66	Glycosyltransferase	CM	OTHER	21.24 ± 0.16
A9WTU3	Penicillin-binding protein	CM	SP	21.23 ± 0.38
A9WQS2	Transcriptional regulator, LytR family	CM	OTHER	21.23 ± 0.42

The MV proteome composition may give hints regarding the function and/or origin of the MVs, as proteins may actively be sorted by an unknown mechanism into MVs or that proteins are in close proximity to the site of MV biogenesis and are therefore detected in the MVs. Therefore, the MV proteome was examined for proteins that belong to the same or similar cellular functions of *R. salmoninarum*. For example, proteins involved in protein transport (A9WP49; A9WP50; A9WSE1; A9WSE2; A9WMN9; A9WST8), glycine betaine transport (A9WPC5; A9WQW0; A9WPC8), amino acid transport (A9WRT5; A9WRT3), oligopeptide transport (A9WPA0; A9WPE4), iron and hemin transport (A9WSK5; A9WMV9; A9WRJ4; A9WRJ5) and other ABC transporters (A9WUM2; A9WM30; A9WPI2; A9WPT7; A9WUY8; A9WNV6; A9WMU4; A9WPM2; A9WQR7) were found in the MVs. Additionally, proteins participating in FeS assembly (A9WT31; A9WT29; A9WT32), cell division (A9WRD6; A9WRE4; A9WTJ9) and other cell wall modifying processes (A9WRF5; A9WTU3; A9WTJ9; A9WLN3; A9WPT9; A9WUR8; A9WU60; A9WRE4; A9WM96; A9WQS2; A9WU75) were detected.

Discussion

In this first proteome analysis of *R. salmoninarum*, the subcellular localizations of 1,674 proteins were reported with semi-quantitative data. The comparison of the composition and abundance of the detected proteins showed that proteins enriched within the subcellular fraction were also *in silico* predicted to be present. While the majority of proteins were detected in more than one subcellular fraction, the protein abundancies between the subcellular fractions varied greatly in most cases. Interestingly, some proteins like the major virulence factor P57/Msa (A9WL54) and a PPIase (A9WSH8) were high abundant in all analyzed subcellular fractions (Fig. 2), indicating an important role of these proteins for the bacterium. The role of PPIases in virulence is not fully understood. Some studies attribute a secondary role to these proteins, as they are involved in folding and secretion of virulence factors as summarized by Unal and Steinert[34]. The FKBP type PPIase A9WSH8 has a high similarity to a FKBP type PPIase of the intracellular pathogen *Legionella pneumophila*. This PPIase of *L. pneumophila* is called macrophage infectivity potentiator (Mip) protein and is reported to potentiate the infection/replication within macrophages[35]. Also, a similar Mip protein was enriched in the MVs of *Neisseria meningitidis*[26], is reported to be involved in the pathogenicity of the bacterium[36] and lead to bactericidal activity in vaccination studies[37]. As *R. salmoninarum* is able to survive and replicate in macrophages[2] and the A9WSH8 protein was found in all of the subcellular fractions in high abundance, the A9WSH8 protein may be a good target for further research.

Other findings, like the high abundance of the 60 kDa chaperonins 1 (A9WMA0) and 2 (A9WN14) in the cytosol, membrane and extracellular fraction was obvious for an intracellular pathogen, as these proteins help to cope with the stressful environment within the host macrophages. Furthermore, two secretory chitin degrading proteins (A9WUI6; A9WV70) were found in abundance. Due to the large amounts of chitin and chitosan outside the gills and skin, it was already hypothesized that these proteins may be important for the bacterial infection[38]. Moreover, the detected serpin (A9WLI2) plays a role in host pathogen interaction as it is known to inhibit host proteases and interact with host serpins[39]. In addition, iron acquisition proteins are very important for pathogens, as the bioavailability is stringently controlled by host proteins. The ferric enterobactin transporter (A9WMV9) and the putative iron(III) dicitrate-binding protein (A9WSK5) may play important roles regarding iron acquisition of *R. salmoninarum* as they were found to be high abundant in the membrane, extracellular and MV fraction. Of the four described hemolysins of *R. salmoninarum*[14], three hemolysins were detected (A9WUP1; A9WUL5; A9WQI5). While the neutral metalloproteinase (A9WUL5) was detected in the extracellular fraction and the hemolysin A (A9WQI5) in the cytosol and membrane fraction, the negative regulator of genetic competence (A9WUP1) was found in all subcellular fractions, indicating its significance for the bacterium.

A group of proteins known for the establishment of the infection of *R. salmoninarum*, are the targets of the sortase A9WTU8, which covalently anchors the target proteins to the peptidoglycan surface. In case of *R. salmoninarum*, sortase targets are implied to play a role in cell adhesion and colonization of the host. It was previously shown that the inhibition of the *R. salmoninarum* sortase (A9WTU8) results in reduction of bacterial adhesion, invasion and replication within chinook salmon embryo cells (CHSE-214)[15]. Three out of the eight putative sortase targets that are described for *R. salmoninarum* by Sudheesh *et al.*[15] were identified in our study (A9WSP9; A9WUW6; A9WQT3), two of them were also identified in the MVs (A9WSP9; A9WUW6). Amongst these sortase targets, the putative peptidase A9WSP9 is of interest as it might be involved in the degradation of the major immunosuppressive protein P57/Msa. It has been described that P57/Msa is a substrate of an unknown putative autologous cell surface associated serine proteinase which has a molecular mass of 100 kDa or greater and is cleaving the P57/Msa protein over time[40]. Interestingly, the putative peptidase A9WSP9 fits this description as it has an alpha/beta hydrolase fold domain, a mass of 101.37 kDa and is anchored to the bacterial cell surface via a LPxTG cell wall anchor motif. In our data it was detected with high abundance in all of the enriched subcellular fractions. However, further experiments are necessary to prove this hypothesis.

The ability of *R. salmoninarum* to produce MVs has been reported recently[41]. Their study reported the packing of the major virulence factors P22 (A9WV24) and P57/Msa (A9WL54) into the MVs of *R. salmoninarum*[41]. Further, cytotoxic effects of the MVs on the salmon head kidney (SHK-1) cell line were shown[41]. The results presented here support the results of Echeverría-Bugueño *et al.*, as P22 and P57/Msa were also found in high abundance in the vesicles. While P57/Msa was high abundant in all subcellular fractions, P22 was only high abundant in the MV and extracellular fraction, indicating that the MVs may have a role in virulence. The association of P57/Msa with the vesicles is noteworthy, because it has been shown that the association with the membrane is crucial for the virulent properties of this protein[7]. However, while the study by Senson *et. al* shows the importance of the cell association of P57/Msa for the virulence, another study reported that nutritional mutant strains with cell associated P57/Msa were avirulent, indicating that next to P57/Msa another yet uncharactarized factor needs to be present for virulence[42]. The protein that was only found within the MVs, the manganese-binding protein A9WVI9, belongs to the adhesin B protein family (InterPro family identifier: IPR006129). Proteins of this family are involved in bacterial adhesion and are enriched in other Gram-positive bacterial MVs[43]. Taken together, these findings support the current knowledge about the cytotoxic effects of the MVs on protein level and give hints for more targeted research regarding the putative involvement of the MVs during the *R. salmoninarum* infection and development of BKD.

While the complete mechanism of MV shedding in Gram-positive bacteria is not fully understood, it is hypothesised that cell wall modifications (e.g. by transpeptidases and autolysins) play a critical role in the formation of MVs[20–22]. The aforementioned manganese-binding protein A9WVI9, which was the

only protein exclusively found in the MVs, has a NlpC/P60 domain. In addition, more proteins of this major class of cell wall hydrolases were found to be high abundant within the MVs (A9WUF0; A9WKY1; A9WKY2), indicating a role of proteins belonging to the NlpC/P60 family during MV biogenesis. Other cell wall modifying proteins found in the MVs were the penicillin binding protein (A9WTU3), the penicillin insensitive transglycosylase (A9WTJ9), the hypothetical transglycosylase (A9WLN3), the peptidoglycan specific endopeptidase (A9WPT9), the D-alanyl-meso-diaminopimelate endopeptidase (A9WUR8), the hypothetical exported protein (A9WU60), the division specific D,D-transpeptidase (A9WRE4), the FtsQ protein (A9WRD6), three proteins belonging to the LytR family (A9WM96; A9WQS2; A9WU75) and the putative endopeptidase LytE (A9WRF5). A study investigating the MV shedding in *Bacillus subtilis* reported that a LytE homologue, next to three other autolysins, was necessary for the MV production of the bacterium. Together, these findings support the hypothesis that cell wall modifying proteins may be involved in the formation of *R. salmoninarum* MVs.

Taken together, we report the subcellular occurrence of 1,674 proteins of *R. salmoninarum* together with their relative abundance. This data can aid as a backbone for more targeted experiments regarding the development of new drugs for the treatment of BKD or the understanding of the disease in the future. The comparison of the 146 proteins identified from the MV fraction with other subcellular fractions showed that there is no continuous quantitative or qualitative correlation with any of them. Therefore, we can conclude that the composition of the MV proteome is unlikely randomly composed due to impurities. Further, we detected an enrichment of lipoproteins in the MV fraction. This may be especially important for a potential new route of vaccine development against BKD, as many bacterial lipoproteins are antigenic and immunoprotective[17]. In addition, vaccines based on liposomes or MVs are promising candidates because they cannot replicate and the proteins are presented in their native membrane environment[30], which is important for their native structure[44]. Moreover, the identification of P57/Msa protein in the MV fraction is interesting as a live vaccination approach with *R. salmoninarum* strains with normal and reduced cell surface presentation of P57/Msa showed the importance for the presence of P57/Msa for the protection during a challenge experiment in Atlantic salmon[42]. As both P57/Msa and P22 were detected in the MVs along with several adhesins and lipoproteins which are putatively immunogenic, utilization of *R. salmoninarum* MVs as a new route for vaccination of fish against BKD is an interesting topic to examine.

Methods

Bacterial strain, cultivation and harvest

The reference strain ATCC 33209 of *R. salmoninarum* was grown in quadruplicates in PYC medium (1% peptone, 1% yeast extract, 0.1% L-cysteine HCl, pH 6.8)[45] in a 15 °C water bath under shaking at 150 rpm for ~145 hours. Bacteria were harvested at an OD_{600} of 2.1 by centrifugation at 10,000 x g for 20 min at 4 °C. The bacterial pellet was used to isolate the cytosolic and membrane protein subcellular fractions. The supernatant was filtered twice using a 0.45 µm bottle-top filter membrane and used to prepare the extracellular and MV protein fractions.

Preparation of cytosolic and membrane protein fractions

After resuspending the pellet in PBS, bacterial cells were disrupted using a Ribolyser set to 6.5 m/s for 4 cycles at 30 s. In between the cycles the suspension was cooled on ice for 5 min. After the last cycle, samples were centrifuged at 5,000 x g for 5 min at 5 °C to dispose the beads and cell debris. Afterwards, the supernatant was ultracentrifuged at 100,000 x g for 1 h at 4 °C. The supernatant contained the proteins referred to as "cytosolic fraction" in this study. The pellet was washed with HEPES (10 mM, pH 7.4) and ultracentrifuged again. The pellet contained the proteins referred to as "membrane fraction" in this study. Prepared fractions were stored at -20 °C.

Preparation of MV protein fraction

The filtered supernatant was concentrated ~20-fold using tangential flow filtration (Äkta flux, GE Healthcare) with a nominal molecular weight cut-off of 100 kDa and ultracentrifuged afterwards at 100,000 x g for 1 h and 4 °C. The pellet was washed in TE buffer (10 mM Tris-HCl, 1 mM EDTA, pH 7.25) and the supernatant was discarded. Subsequently, the MVs were purified by density gradient centrifugation with OptiPrep (60% Iodixanol). The MV containing pellet was resuspended in 2 ml 50% Iodixanol, diluted with a solution of 0.85% NaCl and 60 mM HEPES (pH 7.4). Then, carefully, 1 ml of 40%, 30% and 10% Iodixanol diluted with 0.85% NaCl and 10 mM HEPES (pH 7.4) were carefully layered from the highest to the lowest Iodixanol concentration above the 50% solution layer. The samples were ultracentrifuged in a swing-out rotor at 100,000 x g for 2 h at 4 °C. The third and fourth 1 ml fraction contained the MVs and were transferred into new ultracentrifugation tubes, diluted 5- to 6-fold with TE buffer and ultracentrifuged again. Finally, the pellets of both fractions were pooled in TE buffer, transferred into a new reaction tube and ultracentrifuged again. The MV containing pellet is referred to as "MV fraction" in this study and was stored at -20 °C.

S-Trap protein digestion and peptide fractionation

The S-Trap protein digest was performed according to manufacturer's protocol (ProtiFi) with minor modifications. Briefly, 20 µg of protein of the cytosolic, membrane and MV fraction, determined by BCA assay according to manufacturer's instructions (Thermo Fisher Scientific), was mixed 1:1 with 2x lysis buffer (10% SDS, 100 mM TEAB, pH 7.55). Afterwards, proteins were reduced in 20 mM DTT for 10 min at 95 °C and alkylated in 40 mM IAA for 30 min in the dark. Samples were acidified by addition of phosphoric acid to a final concentration of 1.2% and diluted 1:7 with S-Trap binding buffer (90% methanol, 100 mM TEAB, pH 7.1). The proteins were digested with 1:50 trypsin in 50 mM TEAB for 3 h at 47 °C in S-Trap micro columns and the peptides were eluted from the columns using 50 mM TEAB, followed by 0.1% aqueous acetic acid, and 60% acetonitrile containing 0.1% acetic acid. The peptides were dried using a vacuum centrifuge.

To reduce the sample complexity, cytosolic, membrane and MV samples were fractionated by performing basic reverse phase peptide fractionation as described by the manufacturer (Pierce high pH reversed-phase peptide fractionation kit, Thermo Fisher Scientific). In short, peptides were loaded onto in-house packed C18 micro spin columns (Dr. Maisch HPLC GmbH ReproSil pur C18, pore size 300 Å, particle size 5.0 µm) and eluted in eight fractions with increasing acetonitrile concentrations ranging from 5 to 50% in a high-pH solution (0.1% triethylamine). The eluates of fractions 1 & 5, 2 & 6, 3 & 7 and 4 & 8 were pooled. Peptides were dried using a vacuum centrifuge, resuspended in 20 µl 0.1% acetic acid and stored at -20 °C until LC-MS/MS measurement.

Preparation of the extracellular protein fraction and in-gel digestion

Extracellular proteins were enriched by using StrataClean affinity beads (Agilent) as described before[46]. In brief, 20 µl of primed StrataClean beads were incubated with 10 ml of filtered bacterial culture supernatant in an overhead shaker over-night at 4 °C. On the next day, the bead suspension was centrifuged for 45 min at 10,000 x g and 4 °C. Afterwards, the pellet was dried using a vacuum centrifuge and the proteins separated by SDS-PAGE. The separation was performed with 130 V until the solvent front reached the middle of the gel. The gel was fixated, Coomassie stained, the lanes cut in five pieces of equal size and tryptically digested as previously described[46]. The dried peptides were resuspended in 10 µl *Aq. dest.* and desalinated using C18 ZipTips according to manufacturer's protocol (Merck Millipore). Afterwards, peptides were resuspended in 20 µl 0.1% acetic acid and stored at -20 °C until LC-MS/MS measurement.

Mass spectrometry data acquisition and analysis

Tryptic peptides of the cytosol, membrane, extracellular and MV subcellular fractions were separated on an Easy nLC 1200 liquid chromatography system (Thermo Fisher Scientific) with a reverse-phase C18 column (in-house packed, inner diameter 100 µm, outer diameter 360 µm, length 200 mm, packed with Dr. Maisch ReproSil pur C18, pore size 120 Å, particle size 3.0 µm) and a column oven set to 45 °C. Peptides were loaded with 22 µl of buffer A (0.1% acetic acid) at 400 bar and subsequently eluted with a non-linear 100 min gradient from 1 to 99% buffer B (95% acetonitrile with 0.1% acetic acid) at a constant flow rate of 300 nl/min. Eluting peptides were measured in an Orbitrap Elite mass spectrometer (Thermo Fisher Scientific) in data dependent mode. The MS1 scan was recorded in the orbitrap with a mass window of 300 - 1,700 m/z and a resolution of 60,000. The 20 most intense precursor ions (ions with an unassigned charge or a charge of 1 were excluded) were selected for CID fragmentation with a collision energy of 35%. The resulting MS/MS spectra were measured by the linear ion trap.

The resulting *.raw-files were searched against the UniProt reference proteome of the *R. salmoninarum* strain ATCC 33209 (ID UP000002007, 3,421 protein entries, download 17th August 2020) and the cRAP contaminants list using MaxQuant software (version 1.6.17.0)[47]. For samples of the cytosol, membrane and MV, the search was performed with a maximum of two missed cleavages, oxidation (M) and acetylation (protein N-term) as variable modifications and carbamidomethylation (C) as a fixed modification. The extracellular fraction was searched with a maximum of two missed cleavages, oxidation (M), acetylation (protein N-term) and carbamidomethylation (C) as a variable modification. Proteins were identified with a minimum of 2 peptides per protein group, with one unique peptide. Match between run was enabled in between biological replicates. For protein quantification, unique and razor peptides were used and the label-free quantification (LFQ) calculation was performed separate for each of the enriched subcellular fractions.

Resulting data was analyzed with Perseus software (version 1.6.14.0)[48]. Data was filtered based on hits against the reverse database, identified by site and the contamination list of MaxQuant. Further, only proteins were treated as quantified if a protein group had LFQ intensities in at least 3 out of 4 replicates. LFQ intensities were log2 transformed and for relative comparison normalized by subtraction of the median.

Transmission electron microscopy

For visualization of membrane vesicles, the method according to Thery *et al.*[50] was applied with minor modifications. Briefly, isolated and purified membrane vesicles were fixed with 2% paraformaldehyde in 0.1 M sodium phosphate buffer (pH 7.5) and then allowed to adsorb onto a glow-discharged carbon-coated holey Pioloform film on a 400-mesh grid (Plano GmbH) for 20 min. The grid was then transferred onto two droplets of PBS, onto a droplet of 1% aqueous glutaraldehyde for 5 min, onto eight

droplets of deionized water for 2 min each, and finally onto a drop of methyl cellulose-uranyl acetate (9 parts 2% methyl cellulose mixed with 1 part 4% aqueous glutaraldehyde) for 10 min on ice. After blotting with filter paper the grids were air-dried. All samples were examined with a transmission electron microscope LEO 906 (Carl Zeiss Microscopy GmbH) at an acceleration voltage of 80 kV. For acquisition of the images, a wide-angle dual speed CCD camera Sharpeye (Tröndle) was used, operated by the ImageSP software. Afterwards, all micrographs were edited using Adobe Photoshop CS6.

Data availability

The mass spectrometry proteomics data have been deposited to the ProteomeXchange Consortium via the PRIDE[49] partner repository with the dataset identifier PXD025586.

Reviewer account details:

Project accession: PXD025586

Username: reviewer_pxd025586@ebi.ac.uk

Password: onmRLtvt

References

1. Bandin, I., Ellis, A., Barja, J. & Secombes, C. Interaction between rainbow trout macrophages and *Renibacterium salmoninarum* in vitro. *Fish Shellfish Immunol.* **3**, 25–33 (1993).

2. Gutenberger, S., Duimstra, J., Rohovec, J. & Fryer, J. Intracellular survival of *Renibacterium salmoninarum* in trout mononuclear phagocytes. *Dis. Aquat. Organ.* **28**, 93–106 (1997).

3. Evelyn, T., Ketcheson, J. & Prosperi-Porta, L. Further evidence for the presence of *Renibacterium salmoninarum* in salmonid eggs and for the failure of povidone-iodine to reduce the intra-ovum infection rate in water-hardened eggs. *J. Fish Dis.* **7**, 173–182 (1984).

4. Balfry, S., Albright, L. & Evelyn, T. Horizontal transfer of *Renibacterium salmoninarum* among farmed salmonids via the fecal-oral route. *Dis. Aquat. Organ.* **25**, 63–69 (1996).

5. Wiens, G. Bacterial kidney disease (*Renibacterium salmoninarum*). in *Fish diseases and disorders. Volume 3: viral, bacterial and fungal infections* (eds. Woo, P. T. K. & Bruno, D. W.) 338–374 (CABI, 2011).

6. Evenden, A., Grayson, T., Gilpin, M. & Munn, C. *Renibacterium salmoninarum* and bacterial kidney disease — the unfinished jigsaw. *Annu. Rev. Fish Dis.* **3**, 87–104 (1993).

7. Senson, P. & Stevenson, R. Production of the 57 kDa major surface antigen by a non-agglutinating strain of the fish pathogen *Renibacterium salmoninarum*. *Dis. Aquat. Organ.* **38**, 23–31 (1999).

8. Rhodes, L., Coady, A. & Deinhard, R. Identification of a Third msa Gene in *Renibacterium salmoninarum* and the Associated Virulence Phenotype. *Appl. Environ. Microbiol.* **70**, 6488–6494 (2004).

9. Fredriksen, Å., Endresen, C. & Wergeland, H. I. Immunosuppressive effect of a low molecular weight surface protein from *Renibacterium salmoninarum* lymphocytes from Atlantic salmon (*Salmo salar* L.). *Fish Shellfish Immunol.* **7**, 273–282 (1997).

10. Brynildsrud, O., Gulla, S., Feil, E. J., Nørstebø, S. F. & Rhodes, L. D. Identifying copy number variation of the dominant virulence factors msa and p22 within genomes of the fish pathogen *Renibacterium salmoninarum*. *Microb. Genomics* **2**, e000055; 10.1099/mgen.0.000055 (2016).

11. Wiens, G., Chien, M., Winton, J. & Kaattari, S. Antigenic and functional characterization of p57 produced by *Renibacterium salmoninarum*. *Dis. Aquat. Organ.* **37**, 43–52 (1999).

12. Bethke, J., Arias- Muñoz, E., Yáñez, A. & Avendaño- Herrera, R. *Renibacterium salmoninarum* iron- acquisition mechanisms and ASK cell line infection: Virulence and immune response. *J. Fish Dis.* **42**, 1283–1291 (2019).

13. McIntosh, D. *et al.* Production of putative virulence factors by *Renibacterium salmoninarum* grown in cell culture. *Microbiology* **143**, 3349–3356 (1997).

14. Wiens, G. *et al.* Genome Sequence of the Fish Pathogen *Renibacterium salmoninarum* Suggests Reductive Evolution away from an Environmental *Arthrobacter* Ancestor. *J. Bacteriol.* **190**, 6970–6982 (2008).

15. Sudheesh, P., Crane, S., Cain, K. & Strom, M. Sortase inhibitor phenyl vinyl sulfone inhibits *Renibacterium salmoninarum* adherence and invasion of host cells. *Dis. Aquat. Organ.* **78**, 115–127 (2007).

16. Hutchings, M. I., Palmer, T., Harrington, D. J. & Sutcliffe, I. C. Lipoprotein biogenesis in Gram-positive bacteria: knowing when to hold ’em, knowing when to fold ’em. *Trends Microbiol.* **17**, 13–21 (2009).

17. Nguyen, M. T. & Götz, F. Lipoproteins of Gram-Positive Bacteria: Key Players in the Immune Response and Virulence. *Microbiol. Mol. Biol. Rev.* **80**, 891–903 (2016).

18. Natale, P., Brüser, T. & Driessen, A. J. M. Sec- and Tat-mediated protein secretion across the bacterial cytoplasmic membrane-Distinct translocases and mechanisms. *Biochim. Biophys. Acta - Biomembr.* **1778**, 1735–1756 (2008).

19. Toyofuku, M., Nomura, N. & Eberl, L. Types and origins of bacterial membrane vesicles. *Nat. Rev. Microbiol.* **17**, 13–24 (2019).

20. Toyofuku, M. *et al.* Prophage-triggered membrane vesicle formation through peptidoglycan damage in *Bacillus subtilis*. *Nat. Commun.* **8**, 481; 10.1038/s41467-017-00492-w (2017).

21. Wang, X., Thompson, C. D., Weidenmaier, C. & Lee, J. C. Release of *Staphylococcus aureus* extracellular vesicles and their application as a vaccine platform. *Nat. Commun.* **9**, 1379; 10.1038/s41467-018-03847-z (2018).

22. Abe, K., Toyofuku, M., Nomura, N. & Obana, N. Autolysis- mediated membrane vesicle formation in *Bacillus subtilis*. *Environ. Microbiol.* **23**, 2632–2647 (2021).

23. Ellis, T. N., Leiman, S. A. & Kuehn, M. J. Naturally produced outer membrane vesicles from *Pseudomonas aeruginosa* elicit a potent innate immune response via combined sensing of both lipopolysaccharide and protein components. *Infect. Immun.* **78**, 3822–3831 (2010).

24. Bitto, N. J. *et al. Staphylococcus aureus* membrane vesicles contain immunostimulatory DNA, RNA and peptidoglycan that activate innate immune receptors and induce autophagy. *J. Extracell. Vesicles* **10**, e12080; 10.1002/jev2.12080 (2021).

25. Chatterjee, D. & Chaudhuri, K. Association of cholera toxin with *Vibrio cholerae* outer membrane vesicles which are internalized by human intestinal epithelial cells. *FEBS Lett.* **585**, 1357–1362 (2011).

26. Lappann, M., Otto, A., Becher, D. & Vogel, U. Comparative Proteome Analysis of Spontaneous Outer Membrane Vesicles and Purified Outer Membranes of *Neisseria meningitidis*. *J. Bacteriol.* **195**, 4425–4435 (2013).

27. Lee, E.-Y. *et al.* Gram-positive bacteria produce membrane vesicles: Proteomics-based characterization of *Staphylococcus aureus*-derived membrane vesicles. *Proteomics* **9**, 5425–5436 (2009).

28. Liu, Y., Defourny, K. A. Y., Smid, E. J. & Abee, T. Gram-Positive Bacterial Extracellular Vesicles and Their Impact on Health and Disease. *Front. Microbiol.* **9**, 1502; 10.3389/fmicb.2018.01502 (2018).

29. Coelho, C. *et al. Listeria monocytogenes* virulence factors, including listeriolysin O, are secreted in biologically active extracellular vesicles. *J. Biol. Chem.* **294**, 1202–1217 (2019).

30. Arigita, C. *et al.* Restored functional immunogenicity of purified meningococcal PorA by incorporation into liposomes. *Vaccine* **21**, 950–960 (2003).

31. Yu, N. Y. *et al.* PSORTb 3.0: Improved protein subcellular localization prediction with refined localization subcategories and predictive capabilities for all prokaryotes. *Bioinformatics* **26**, 1608–1615 (2010).

32. Almagro Armenteros, J. J. *et al.* SignalP 5.0 improves signal peptide predictions using deep neural networks. *Nat. Biotechnol.* **37**, 420–423 (2019).

33. O'Farrell, C. L., Elliott, D. G. & Landolt, M. L. Mortality and kidney histopathology of chinook salmon *Oncorhynchus tshawytscha* exposed to virulent and attenuated *Renibacterium salmoninarum* strains. *Dis. Aquat. Organ.* **43**, 199–209 (2000).

34. Unal, C. M. & Steinert, M. Microbial Peptidyl-Prolyl cis/trans Isomerases (PPIases): Virulence Factors and Potential Alternative Drug Targets. *Microbiol. Mol. Biol. Rev.* **78**, 544–571 (2014).

35. Cianciotto, N. P. & Fields, B. S. *Legionella pneumophila* mip gene potentiates intracellular infection of protozoa and human macrophages. *Proc. Natl. Acad. Sci. U. S. A.* **89**, 5188–5191 (1992).

36. Reimer, A. *et al.* Inhibitors of macrophage infectivity potentiator-like PPIases affect neisserial and chlamydial pathogenicity. *Int. J. Antimicrob. Agents* **48**, 401–408 (2016).

37. Costoya, L., Marzoa, J., Ferreirós, C. & Criado, M. T. Liposomes or traditional adjuvants: induction of bactericidal activity by the macrophage infectivity potentiator protein (Mip) of *Neisseria meningitidis*. *APMIS* **125**, 725–731 (2017).

38. Xing, P., Liu, D., Yu, W. G. & Lu, X. Molecular characterization of an endo-type chitosanase from the fish pathogen *Renibacterium* sp. QD1. *J. Mar. Biol. Assoc. United Kingdom* **94**, 681–686 (2014).

39. Bao, J. *et al.* Serpin functions in host-pathogen interactions. *PeerJ* **6**, e4557; 10.7717/peerj.4557 (2018).

40. Rockey, D. D., Turaga, P. S. D., Wiens, G. D., Cook, B. A. & Kaattari, S. L. Serine proteinase of *Renibacterium salmoninarum* digests a major autologous extracellular and cell-surface protein. *Can. J. Microbiol.* **37**, 758–763 (1991).

41. Echeverría- Bugueño, M., Balada, C., Irgang, R. & Avendaño- Herrera, R. Evidence for the existence of extracellular vesicles in *Renibacterium salmoninarum* and related cytotoxic effects on SHK- 1 cells. *J. Fish Dis.* **44**, 1015–1024 (2021).

42. Daly, J. G., Griffiths, S. G., Kew, A. K., Moore, A. R. & Olivier, G. Characterization of attenuated *Renibacterium salmoninarum* strains and their use as live vaccines. *Dis. Aquat. Organ.* **44**, 121–126 (2001).

43. Codemo, M. *et al.* Immunomodulatory effects of pneumococcal extracellular vesicles on cellular and humoral host defenses. *MBio* **9**, 559–577 (2018).

44. Thoma, J. *et al.* Protein-enriched outer membrane vesicles as a native platform for outer membrane protein studies. *Commun. Biol.* **1**, 23; 10.1038/s42003-018-0027-5 (2018).

45. Daly, J. & Stevenson, R. Nutrient Requirements of *Renibacterium salmoninarum* on Agar and in Broth Media. *Appl. Environ. Microbiol.* **59**, 2178–2183 (1993).

46. Bonn, F. *et al.* Picking Vanished Proteins from the Void: How to Collect and Ship/Share Extremely Dilute Proteins in a Reproducible and Highly Efficient Manner. *Anal. Chem.* **86**, 7421–7427 (2014).

47. Tyanova, S., Temu, T. & Cox, J. The MaxQuant computational platform for mass spectrometry-based shotgun proteomics. *Nat. Protoc.* **11**, 2301–2319 (2016).

48. Tyanova, S. *et al.* The Perseus computational platform for comprehensive analysis of (prote)omics data. *Nat. Methods* **13**, 731–740 (2016).

49. Perez-Riverol, Y. *et al.* The PRIDE database and related tools and resources in 2019: improving support for quantification data. *Nucleic Acids Res.* **47**, D442–D450 (2019).

50. Théry, C., Amigorena, S., Raposo, G. & Clayton, A. Isolation and Characterization of Exosomes from Cell Culture Supernatants and Biological Fluids. *Curr. Protoc. Cell Biol.* **30**; 10.1002/0471143030.cb0322s30 (2006).

Figure legends

Figure 1: Overview of the protein identifications, predicted protein localizations and predicted signal peptides for all enriched subcellular fractions: (A) Principal component analysis of the enriched subcellular fractions. Missing values were imputed from normal distribution of each replicate (MV = membrane vesicle); (B) Overview of the overlap and the exclusively quantified proteins between the four enriched subcellular fractions (MV = membrane vesicle); (C) Illustration of the summed LFQ intensities of quantified proteins in the four subcellular fractions assigned to the respective predicted PSORTb localizations. The number of quantified proteins with the respective PSORTb prediction in each of the subcellular fractions is indicated above the bars; (D) Illustration of the summed LFQ intensities of quantified proteins in the four subcellular fractions assigned to the predicted SignalP protein signal peptides. The number of quantified proteins with the respective SignalP signal peptide prediction within the subcellular fractions is indicated above the bars.

Figure 2: Schematic visualization of 25 high abundant proteins that are involved in virulence processes of *R. salmoninarum* and their experimental subcellular localization. Proteins are colored depending on their high abundance (higher than a log2 transformed median normalized LFQ intensity of 2) in one or more of the enriched subcellular fractions. Proteins are marked with their UniProt identifier.

Figure 3: Transmission electron micrographs of isolated and purified membrane vesicles of *R. salmoninarum*.

Competing interests

The authors have no other relevant affiliations or financial involvement with any organization or entity with a financial interest in or financial conflict with the subject matter or materials discussed in the manuscript apart from those disclosed.

Acknowledgements

This work is supported by the European Maritime and Fisheries Fund and the federal state Mecklenburg-Vorpommern [grant MV-II.1-LM-003/730217000003]. We thank Annette Meuche for excellent technical assistance with TEM.

Author contributions

Conceptualization, T.K. and D.B.; methodology, T.K.; formal analysis, T.K. and D.F.; investigation, T.K..; writing—original draft preparation, T.K.; writing—review and editing, A.T.-S., B.K., D.B.; visualization, T.K.; supervision, B.K. and D.B.; project administration, A. T.-S.; funding acquisition, B.K. and D.B. All authors have read and agreed to the published version of the manuscript.

Supplementary Files

This is a list of supplementary files associated with this preprint. Click to download.

- Supplementarytable.xlsx